Auxetic Composites Made of 3D Textile Structure and Polyurethane Foam

Lin Zhou, Jiang Lili, Hong Hu*

Institute of Textiles and Clothing, The Hong Kong Polytechnic University, Hung Hom, Kowloon, Hong Kong

*Corresponding author: tchuhong@polyu.edu.hk

Abstract

Auxetic composites have attracted considerable attention in recent years and have demonstrated a high potential of applications in different areas due to their wonderful properties as compared to non-auxetic composites. In this study, a three-dimensional (3D) auxetic textile structure previously developed was used as reinforcement to fabricate auxetic composites with conventional polyurethane (PU) foam. Both the deformation behavior and mechanical properties of the auxetic composites under compression were analyzed and compared with those of the pure PU foam and non-auxetic composites made with the same materials and structural parameters but with different yarn arrangement. The results show that the negative Poisson's ratio of composites can be obtained when suitable yarn arrangement in a 3D textile structure is adopted. The results also show that the auxetic composites and non-auxetic composites have different mechanical behaviors due to different yarn arrangements in 3D textile structure. While the auxetic composites behave more like damping material with lower compression stress, the non-auxetic composite behaves more like stiffer material with higher compression stress. It is expected that this study could pave a way to the development of innovative 3D auxetic textile composites for different potential applications such as impact protection.

Keywords: Auxetic composite, 3D auxetic textile structure, Negative Poisson's ratio, Compression behavior

1. Introduction

Auxetic materials are a special type of materials that exhibit negative Poisson's ratio (NPR). They laterally bulge when stretched or laterally shrink when compressed [1]. Although Lakes first produced isotropic PU foam materials with a Poisson's ratio value of -0.7 by using a non-auxetic open-cell structure through volumetric compression and heating process in 1987 [2], some theoretical works on NPR [3-4] had been undertaken before. Since then, more efforts have been made to discover, propose, predict, and develop new auxetic structures and materials based on different material scales. The examples include auxetic fibres [5-7], auxetic fabrics [8-13], auxetic foams [14-21], and auxetic composites [22-25]. At the same time, theoretical and simulation works on some fundamental auxetic structures and mechanisms at nano-scale and micro-scale such as hexamer molecules [26], cubic metals [27], graphene [28], silicates [29] and partial auxeticity [30] have also been done. Anomalous behaviours such as locally negative stiffness and compliance in constrained auxetic plates in three-dimension and two-dimension have also been reported [31-32]. In recent years, auxetic materials continue to gain increasing research interests due to their counter-intuitive behaviour [33]. With such unique behaviours, auxetic materials have been shown to provide some remarkable benefits, including fracture toughness, synclastic curvature, enhanced energy absorption ability, and indentation resistance, which make them considerably outperform non-auxetic

materials with various potential applications [31, 34].

Auxetic foams could be fabricated from conventional foams through a process involving compression, heating, cooling [2]. Recently another manufacturing method has been suggested by Grima et al. based on the use of solvents [35]. As a particular kind of auxetic materials, the development of auxetic composites has currently attracted a great attention due to their potential application in protection such as helmets and cushions, aerospace and automotive industry [36], etc. In 1992, Milton [37] already proposed the possibilities of fabricating composite laminates with auxetic value near to '-1'. Presently, there are mainly two methods for fabricating auxetic composites, either from conventional components via specially designed configurations [23, 38-39] or from auxetic components [40]. The conventional manufacturing method is to utilize unidirectional layers of carbon fibre reinforced epoxy stacked in specific sequences [41] exhibiting in-plane [42] or out of plane NPRs [38, 43]. The Poisson's ratio value of composites produced with this method is between -0.21 and -0.37 when the angle of laminates ranges from ±15° to ±30° [44]. A further method of fabricating auxetic composites is to make an auxetic structure by using non-auxetic fibres. In 1992, Evans et al. [45] successfully modelled auxetic effect in network-embedded composites. Chen and Lakes [40] investigated the viscoelastic properties of composite made of non-auxetic and re-entrant auxetic foam as a matrix. Alderson et al. [25] showed that utilizing auxetic fibres as reinforcement exhibit better mechanical properties than other auxetic composites, because enhancing the interface strength of the matrix and fibres enables the composites to bear more

than twice the maximum load. Miller et al [46] reported the fabrication of auxetic composites using a woven auxetic fabric manufactured from auxetic yarns. Recently, auxetic textile structures have also been developed for composite reinforcement. One of the examples is a 3D auxetic textile structure developed by Ge, Hu et al. [9-10, 47] from a 3D orthogonal woven structure by regularly eliminating reinforcing yarns in one direction of the fabric structure. This innovative 3D auxetic textile structure has similar mechanism to the nodule fibril mechanism used to explain auxetic effect in microporous polymers studied by Alderson et al. [48]. Both types of structures could result in positive and negative strain-dependent Poisson's ratios when compressed. By eliminating the stitch yarn in this 3D auxetic textile structure, Jiang, Hu et al. [24] recently proposed a new process to fabricate auxetic composite using multilayer orthogonal auxetic structure as reinforcement and polyurethane (PU) foam as matrix. Based on the compression testing results, they found that the auxetic composite had an obvious auxetic effect under compression. However, as the stitch yarns were not used in the auxetic multilayer orthogonal structure, the delamination of composite structure could happen under impact load.

This work aimed to study a novel type of auxetic composites using the same type of 3D auxetic textile structure proposed in [9-10] as reinforcement and non-auxetic PU foam as matrix. The 3D textile structures were first produced on a prototype machine specially developed by varying their warp yarn diameter and arrangement. Then, composites were fabricated using an injection and foaming process. The composites were finally tested under different compression conditions to assess their deformation

behaviour and mechanical properties. It is expected that this study could pave a way to the development of innovative 3D auxetic textile composites for different potential applications such as impact protection.

2 Experimental

2.1 Design and fabrication of 3D auxetic textile structure

3D auxetic textile structure used in this study was designed based on the modification of a 3D orthogonal woven structure by regularly eliminating reinforcing yarns in one fabric direction [9-10]. As shown in Figure 1(a), the structure consists of three yarn systems, namely weft yarns in the x direction, warp yarns in the y direction and stitch yarns in the z direction. The weft and warp yarns are used as reinforcing yarns. They are alternately arranged layer by layer in two orthogonal directions of the fabric plane (x-y plane) and are bound together by the stitch yarns through the fabric thickness direction (z direction) to form an integrated fabric structure. Another objective of using the stitch yarns is to avoid the possible delamination of the structure. The cross-sections of the structure in x-y plane, x-z plane and y-z plane are shown in Figure 1(b), (c) and (d), respectively. A small part of amplified structure is also shown in Figure 1(c) to get a better view. At the unloaded state, both the weft and warp yarns are in a straight state. In order to achieve auxetic effect in the x-z plane, as shown in Figure 1(c), the warp yarns are regularly eliminated in each warp yarn layer to create void spaces. As shown in Figure 2(a), due to the void spaces created by elimination of the warp yarns, the weft yarns will crimp by action of the warp yarns under compression, resulting in shrinking of the structure in the x-z plane. As a result,

auxetic effect is achieved. Unlike the arrangement of warp yarns, the weft yarns are arranged in each and every weft yarn layer without any elimination. In this case, the warp yarns can keep straight state under compression due to support of the weft yarns. Therefore, the 3D auxetic structure will have NPR in the x-z plane and zero Poisson's ratio in the y-z plane for loading in the z direction.

In order to make the comparison, 3D textile structure with different warp yarn arrangement is also included in this study. As shown in Figure 2(b), as the warp yarns are arranged in the form of vertical lines in the loading direction and the distance between two adjacent warp yarns S_x are kept unchanged, the weft yarn will not be crimped under compression. In this case, the misalignment of the warp yarns could happen with the increase of compression strain.

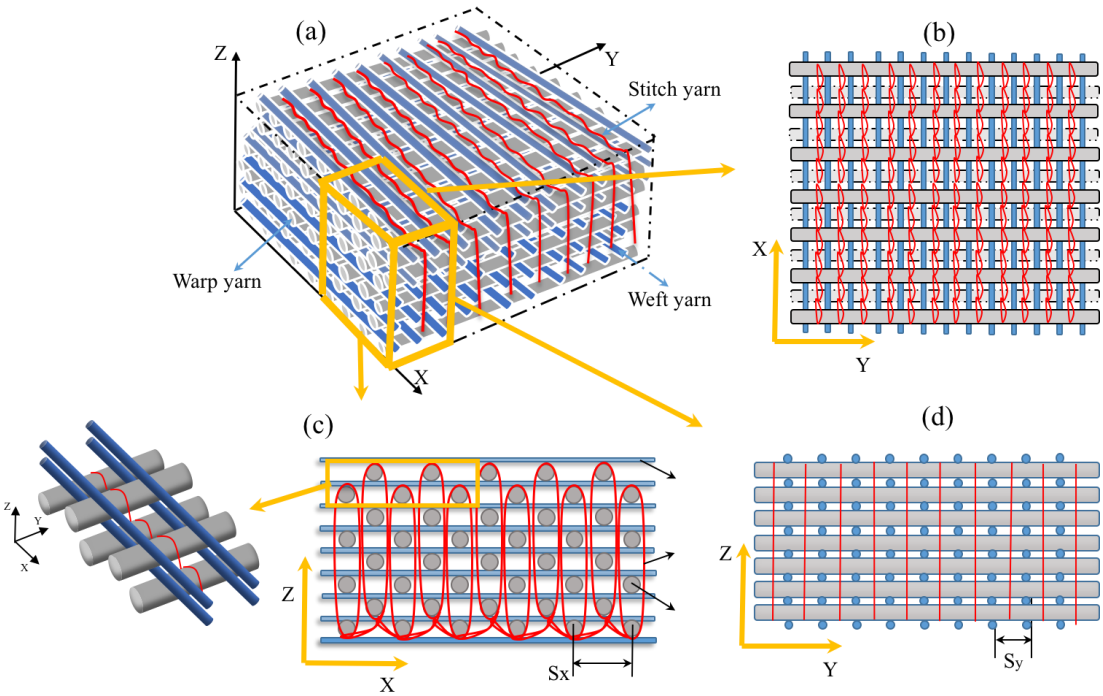

Figure 1 3D auxetic textile structure: (a) 3D view; (b) x-y cross-section; (c) x-z cross-section; (d) y-z cross section.

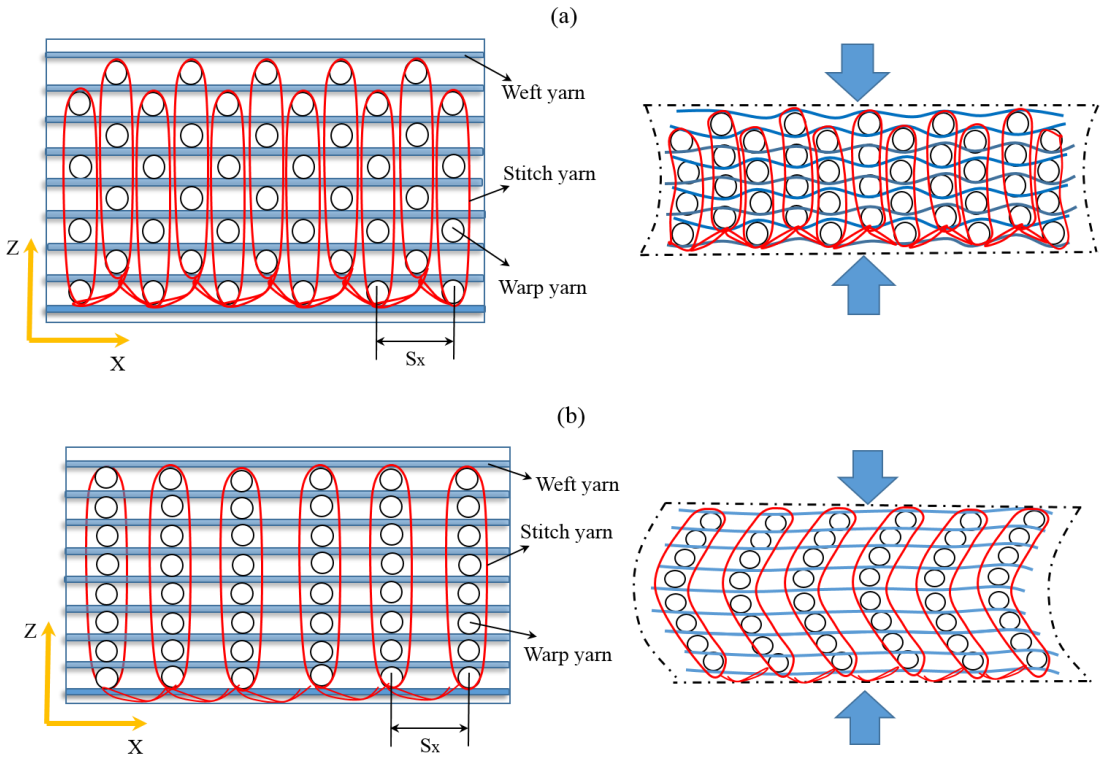

Figure 2 Deformation of 3D textile structures under compression: (a) auxetic structure; (b) non-auxetic structure.

A prototype machine was built to fabricate the above designed 3D auxetic and non-auxetic textile structures [49]. The process includes two steps. The first step is to place the weft and warp yarns in a mold made of stainless steel as shown in Figure 3. The second step is to stitch the weft and warp yarns together to form a 3D integrated textile structure. The difference in the fabrication of auxetic and non-auxetic structures is the result of different placements of the warp yarns in the mold. In order to easily achieve NPR of the auxetic structure, rigid braided yarns made of polyamide fiber were used as the warp yarn, and flexible braided cotton yarn was used as the weft yarn. Polyester multifilament was used as stitching yarn to bind the warp and weft yarns together. To facilitate the comparison, the space between two adjacent weft yarns (weft yarn spacing S_y) and that between two adjacent warp yarns (warp yarn

spacing S_x), as shown in Figure 1(c) and (d), were kept unchanged for both the auxetic structure and non-auxetic structure, respectively. Previous studies [9-10] have shown that a high size difference between the warp and weft yarns could achieve higher auxetic effect of the auxetic structure. For this reason, warp yarns with a much larger diameter than that of the weft yarns were used for fabricating the auxetic textile structure. Table 1 lists the structural parameters of both the auxetic and non-auxetic structures fabricated. It should be noted that except the difference in the arrangement of the warp yarns, all the structural parameters were kept the same for the auxetic and non-auxetic structures.

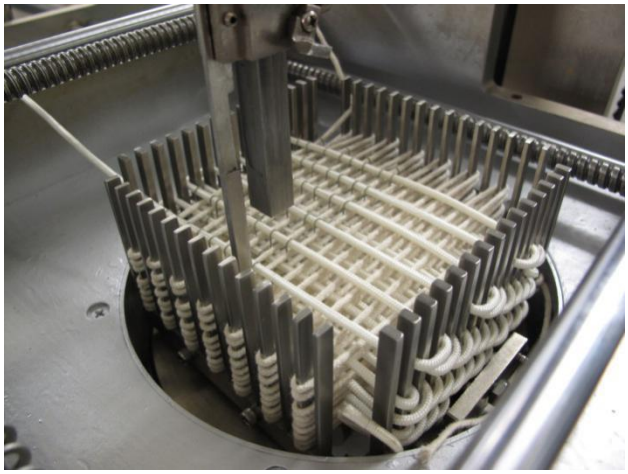

Figure 3 Fabrication of 3D auxetic textile structure on a prototype machine.

Table 1 Structural parameters of auxetic and non-auxetic structures

Fabric structure	Diameter of weft yarn (mm)	Diameter of warp yarn (mm)	Diameter of stitch yarn (mm)	Weft yarn spacing S_y (mm)	Warp yarn spacing S_x (mm)	Fabric structure thickness (mm)
Auxetic (4mm)	2	4	0.5	7.5	15	46
Non-Auxetic (4mm)	2	4	0.5	7.5	15	46
Auxetic (6mm)	2	6	0.5	7.5	15	50
Non-Auxetic (6mm)	2	6	0.5	7.5	15	50

2.2 Fabrication of composites

Both auxetic and non-auxetic composites were fabricated using the 3D textile structures above fabricated as reinforcement and PU foam as matrix via an injection and foaming process. The fabrication process is shown in Figure 4. In order to keep all the weft yarns and warp yarns in a straight state, 3D textile structure fixed together with the stainless steel mold (Figure 4(a)) was first placed into a mold made of Polytetrafluoroethene (PTFE) (Figure 4(b)). Then, the chemical solution, which was uniformly mixed with two chemical constitutes PU resin composition and MDI (isocyanate), was injected into the PTFE mold (Figure 4(c)) to form the PU foam (Cst-1076A/B) in the presence of a blowing agent. The PU resin composition contains ingredients including polyether polyol, catalysts and blowing agents. The general technical indicators of Cst-1076A/B PU foam are listed in Table 2. All chemical materials were of analytical grade and used as received without further purification. After injection, the mold was closed to let the foaming process to occur. After finishing the foaming process, the composite was de-molded from the mold and cut to the required size for the subsequent compression tests. Four types of composites including two auxetic composites made of structures Auxetic (4mm) and Auxetic (6mm), named as 4mm NPR and 6mm NPR, and two non-auxetic composites made of structures Non-auxetic (4mm) and Non-auxetic (6mm), named as 4mm PPR and 6mm PPR, were finally obtained. For comparison purpose, the pure PU foam was also fabricated. Some of the produced samples including the pure PU foam, the auxetic composite 6mm NPR and non-auxetic composite 6mm PPR are shown in Figure 5

(a)-(c), respectively.

Table 2 General technical indicators of Cst-1076 A/B PU foam

	A	B
Composition	polyether polyol	Isocyanate
Color	Ivory	blackened brown
Blending Ratio	100	30-40
Foaming Ratio (%)	15-20	
Foam Density (kg/m^3)	32-35	
Tensile Strength (/k pa)	60-118	
Tear Strength (/N/cm)	2.8-8.6	
Rebound Rate (%)	26-60	

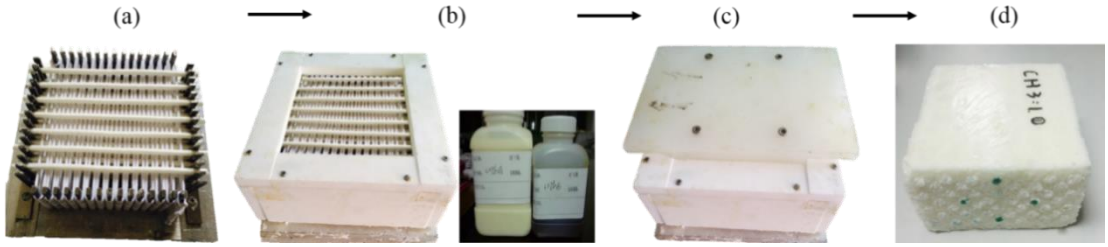

Figure 4 Fabrication process of composites.

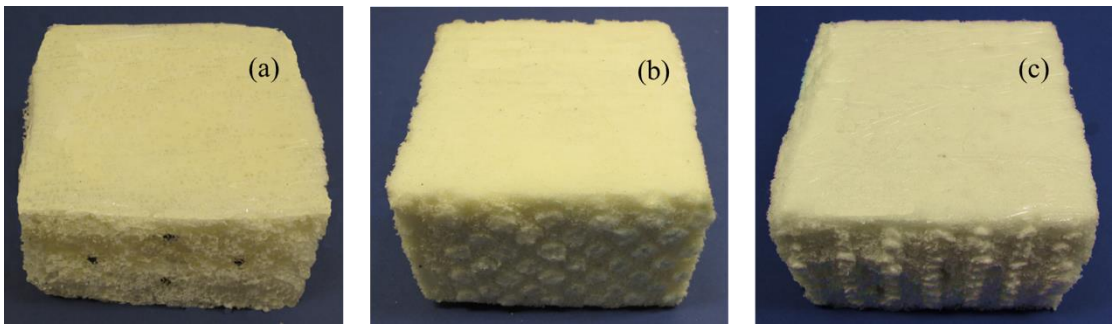

Figure 5 Samples produced: (a) pure PU foam; (b) auxetic composite; (c) non-auxetic composite.

2.3 Compression tests

The pure PU foam, auxetic and non-auxetic composites above produced were subjected to the compression tests in order to assess their deformation behavior and mechanical properties. The testing device used was an Instron 5566 Universal Testing

Machine (Instron Worldwide Headquarters, Norwood, Massachusetts, USA) equipped with two 150mm circular compression plates. The set-up of the testing system is shown in Figure 6. All the compression tests were carried out at a compression speed of 30mm/min up to a 55% deformation of the initial thickness of each sample. The maximum load of the testing device and the sample size were 10kN and 10cm x 10cm, respectively. Three samples were used for each type of material and the mean value was calculated. In order to measure the axial and transversal size changes of sample, as show in Figure 6, four black points were marked on the cross-section of each sample to facilitate recording of the deformation information during compression process. A camera Canon PowerShot G10 with a timer shot function, which was placed at a distance of 50 cm from the sample, was used to take pictures of the marked points. The initial distances between the marked points in both the horizontal and vertical directions were first measured before compression. As shown in Figure 6, H is the distance between the two marked points in the vertical direction and L is the distance between the two marked points in the horizontal direction. H_0 and L_0 are their initial values. The distances of the marked points were measured from the pictures taken by the camera during the compression process using a screen ruler. Based on the measured results, the compression strain ε_z and transversal strain ε_x could be calculated from Eq. (1) and (2).

$$\varepsilon_z = \frac{H - H_0}{H_0} \tag{1}$$

$$\varepsilon_x = \frac{L - L_0}{L_0} \tag{2}$$

Finally, Poisson's ratio ν could be calculated from Eq. (3).

$$v = -\frac{\varepsilon_x}{\varepsilon_z} \tag{3}$$

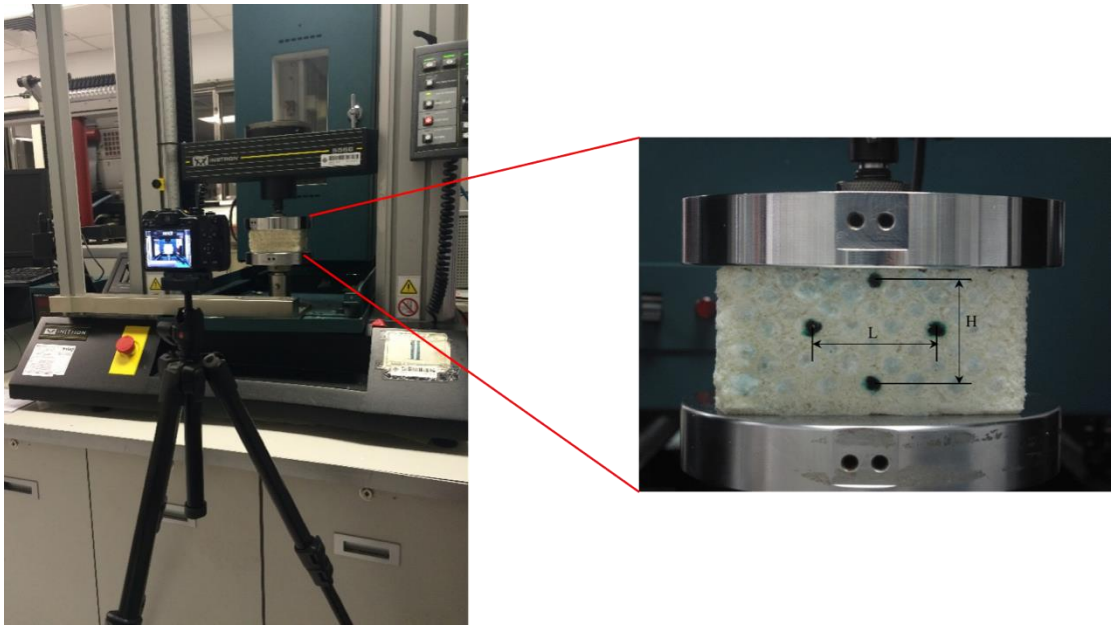

Figure 6 Set-up of the testing system.

One of the problems to be encountered by an auxetic textile composite is the loss of its auxetic behavior and mechanical properties under repeating compression conditions, which will affect its performance during repeated uses. In order to understand how the produced 3D auxetic composite samples could keep their auxetic behavior and mechanical properties, a repeating compression test was also conducted. The compression cycles used were ten. A pre-load of 0.2N was applied at the start of each cycle. For each compression cycle, the composite was first compressed to a 55%

deformation related to its initial state at a speed of 30 mm/min and kept at this deformation for 2 seconds, and then released to its initial position with the same speed and kept for 5 seconds at this position.

3. Results and discussion

3.1 Deformation behavior

The Poisson's ratios as a function of the compression strain calculated from the experimental result for all three types of materials, namely the pure PU foam, the auxetic composites and the non-auxetic composites, are shown in Figure 7. It can be seen that the Poisson's ratio values of three types of materials are not constant with the increase of compression strain and that the quasi-zero Poisson's ratio phenomenon exists for all three types of materials in the initial stage of compression process. For the pure PU foam, its Poisson's ratio is about zero from 0% to 5% of compression strain and reaches a maximum value of 0.103 at the compression strain of 10%. After then, its Poisson's ratio starts to decrease slightly, but still above zero. For the non-auxetic composites, their Poisson's ratios are about zero from 0% to 9% of compression strain and then start to increase but the values do not exceed 0.026. For the auxetic composites, their Poisson's ratios are about zero from 0% to 5% of compression strain, and then become negative. It is found that their NPR values first increase with the increase of the compression strain up to 35%, then start to slightly decrease up to 55%. It is also found that larger diameter of the warp yarns can result in higher NPR values. This quasi-zero Poisson's ratio phenomenon has been

confirmed in our previous study [24]. For the self-made pure PU foam, it has the quasi-zero Poisson's ratio in the initial stage of compression due to its particular porous structure. In this stage, the compression mainly causes the decrease of voids sizes in the compression direction, and not in the transversal direction. As a result, the size of the pure foam in the transversal direction almost keeps unchanged. For the auxetic and non-auxetic composites, as the gaps between each layer of textile reinforcements and the peripheries of the reinforcements are filled with the PU foam, and at the same time, the compressive modulus of PU foam is much lower than that of the braided cotton yarn and braided polyamide yarn, their deformation in the initial stage of compression process mainly comes from the deformation of the PU foam. As the pure PU foam has quasi-zero Poisson's ratio in the initial stage of compression process, the auxetic and non-auxetic composites have also quasi-zero Poisson's ratio in this stage. However, with the increase of the compression strain, the PU foam starts to be compact and the deformation of composites mainly comes from the textile reinforced structure. As explained above, for the auxetic composites, the weft yarns will crimp under compression because of the void spaces created by elimination of the warp yarns. But for the non-auxetic composites, the warp yarns are arranged in each and every layer without any elimination, which can support all the weft yarns to be kept in the straight state under compression. Therefore, the NPRs are obtained for the auxetic composites reinforced with 3D auxetic textile structure and the positive Poisson's ratios are obtained for the non-auxetic composites reinforced with non-auxetic textile structure. The results clearly show that textile structure plays a

vital role in the deformation behavior of the composites.

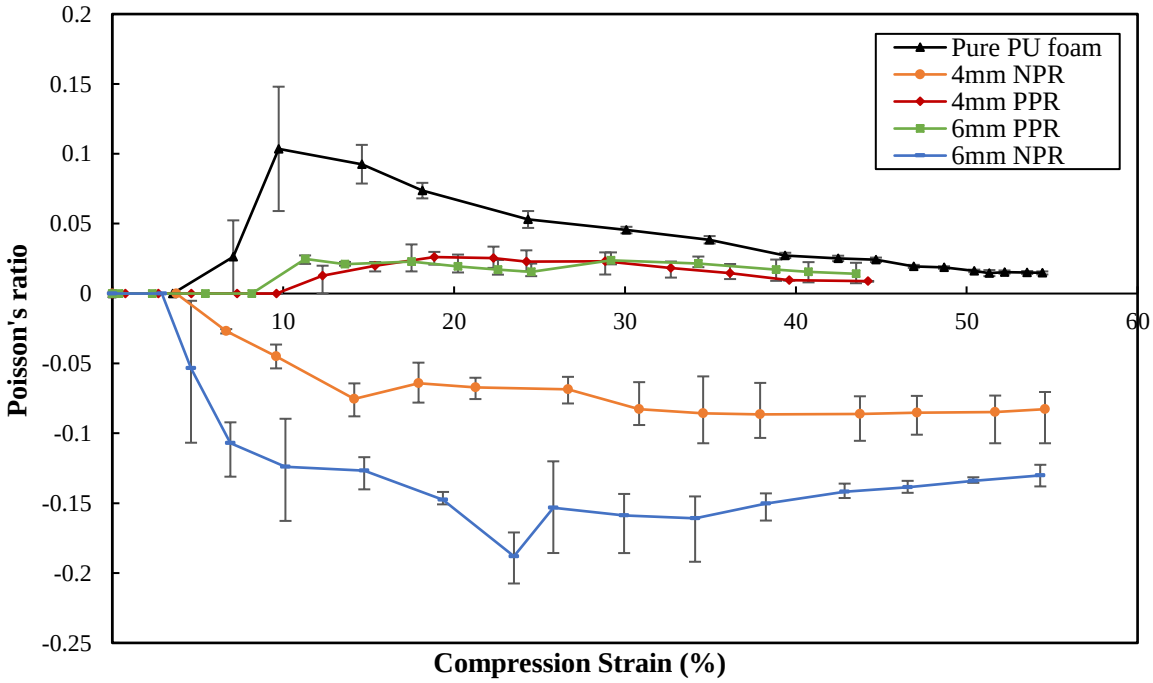

Figure 7 Poisson's ratio-compression strain curves of pure PU foam, auxetic composite and non-auxetic composites

Figure 8 and Figure 9 show the lateral deformations of 6mm NPR auxetic composite and 6mm PPR non-auxetic composite under compression. From Figure 8, it can be seen that the auxetic composite laterally contracts under compression. This effect comes from the crimping of the weft yarns in the x-z plane as shown in Figure 2(a). On going from (a) to (c) of Figure 8, with the increase of the compression strain, the weft yarns get more crimped, resulting in an increase of shrinkage of the composite, and thus an increase of NPR values. However, on going from (c) to (d) of Figure 8, the NPR values start to slightly decrease from 35% to 55% of compression strain because the void spaces of auxetic composites are gradually filled under compression. Although the value of L increases from (c) to (d) of Figure 8, the value of L is still

smaller than that of L_0, indicating the composite still has the NPR effect, but with a decrease of NPR values. Moreover, an increase of the warp yarn diameter allows a larger displacement of the weft yarns in the compression direction, causing a higher shrinking of the composite at the same compression strain. Therefore, increasing the diameter of the warp yarns can also result in an increase of auxetic behavior of the composite. However, for the non-auxetic composites, the influence of the yarn diameter on the Poisson's ratio is not very evident. As shown in Figure 2(b), as all warp yarns are arranged in the form of vertical lines in the loading direction, the weft yarns can keep a straight form under compression. As shown in Figure 9, at the lower compression strains under 9%, as the warp yarns which are arranged in the form of vertical lines well support the weft yarns and the weft yarns cannot be crimped, the Poisson's ratios of composites are quasi-zero. However, after the compression ratio exceeds 9%, on one hand, the cross-section of the warp yarns changes from the circular form to the elliptic form with increased compression stress; on the other hand, the warp yarns arranged in vertical lines start to lose their stability and the warp yarns located in the central layer shift towards the left or right side of the composite, causing an increase of composite size along the horizontal direction in x-z plane. As a result, the Poisson's ratio values become positive. The above analyses indicate that although the auxetic and non-auxetic composites were made with the same materials and the same structural parameters, their deformation behaviors are completely different because of the different arrangements of the warp yarns in the 3D textile structure. While the auxetic composites have NPRs with a very stable composite

structure, the non-auxetic composites have zero and positive Poisson's ratios with instable composite structure.

In order to know the experimental errors, the error bars are also inserted in Figure 7 for each Poisson's ratio value. In the initial stage of compression strain, the error range is relatively large for three types of materials. With compacting of the PU foam, their Poisson's ratio values tend to become relatively stable. The largest standard deviations for composites 4mm NPR, 6mm NPR, 4mm PPR, 6 mm PPR and PU foam are 1.9%, 4.1%, 0.9%, 0.9% and 4.4% respectively, which all happened between 0% and 20% of compression strain except for 4mm NPR that happened at 33% of compression strain. For the pure PU foam, the error ranges are much higher at lower compression strain due to the non-uniform distributions of voids in its structure. However, with the increase of the compression strain, the PU foam is getting compact and the error ranges decrease. For the non-auxetic composites, as the compression loads are mainly supported by the warp yarns and the variations in the measurement of the deformation of the cross section of the warp yarns is smaller, lower errors of the results are obtained. For the auxetic composites, they have a wider range of error than that of non-auxetic composites. Although the three samples of each type of auxetic composite are fabricated and tested in the same experimental condition, there are avoidable differences in their NPRs coming from factors such as voids in the self-fabricated PU foams, the gaps between the warp yarns and weft yarns in inner auxetic structures, the deformation process of inner 3D auxetic structures due to crimping of weft yarns under compression, etc.

Compared with the nodule-fibril (NF) model proposed by Alderson et al. [49], the results obtained for the auxetic composites in this study have the similar trends, that is, the NPR values increase with the increase of compression strain in the first stage of compression process, because both structures have the similar deformation mechanisms as explained before. In the second and third stage of the NF model, the Poisson's ratio curve shows a steep increase to zero before achieving a plateau with positive values. Although the changes of Poisson's ratio from negative to zero and then even to positive have not been observed in the present study due to limitation of experimental condition, it is expected that the same phenomenon could be obtained if auxetic composites continue to be compressed to a much high compression strain.

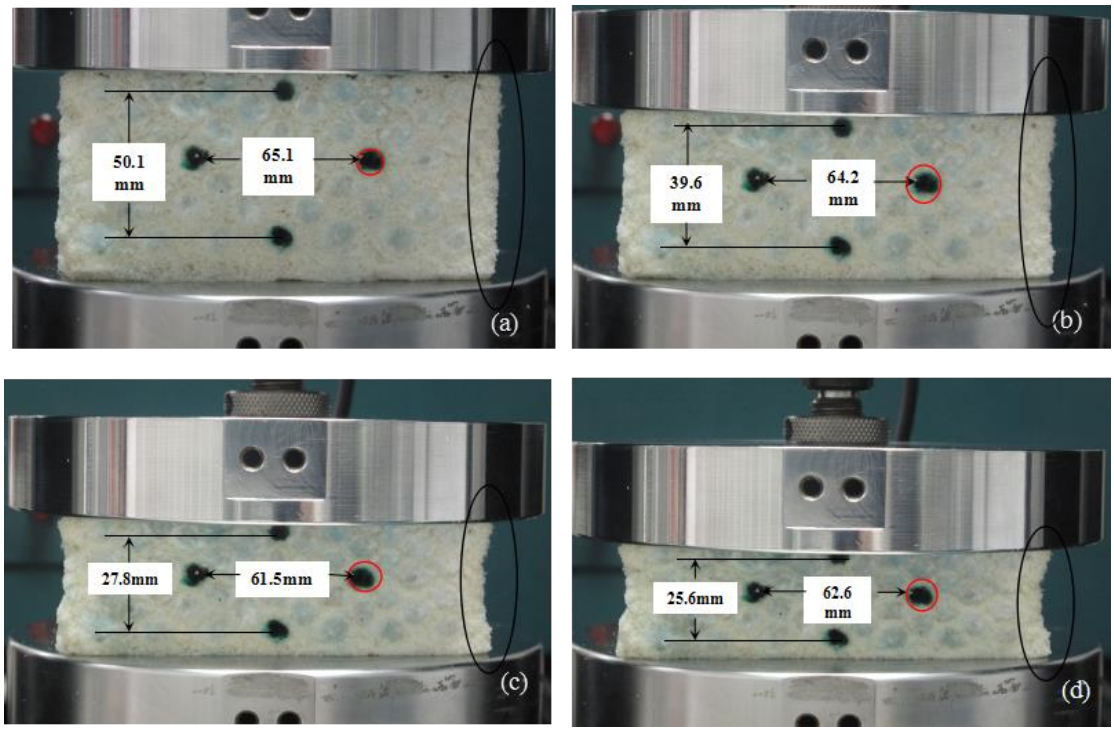

Figure 8 Lateral deformation of 6mm NPR auxetic composite under compression. Compression strain: (a) 0%; (b) 13.450%; (c) 35.98%; (d) 54.36%

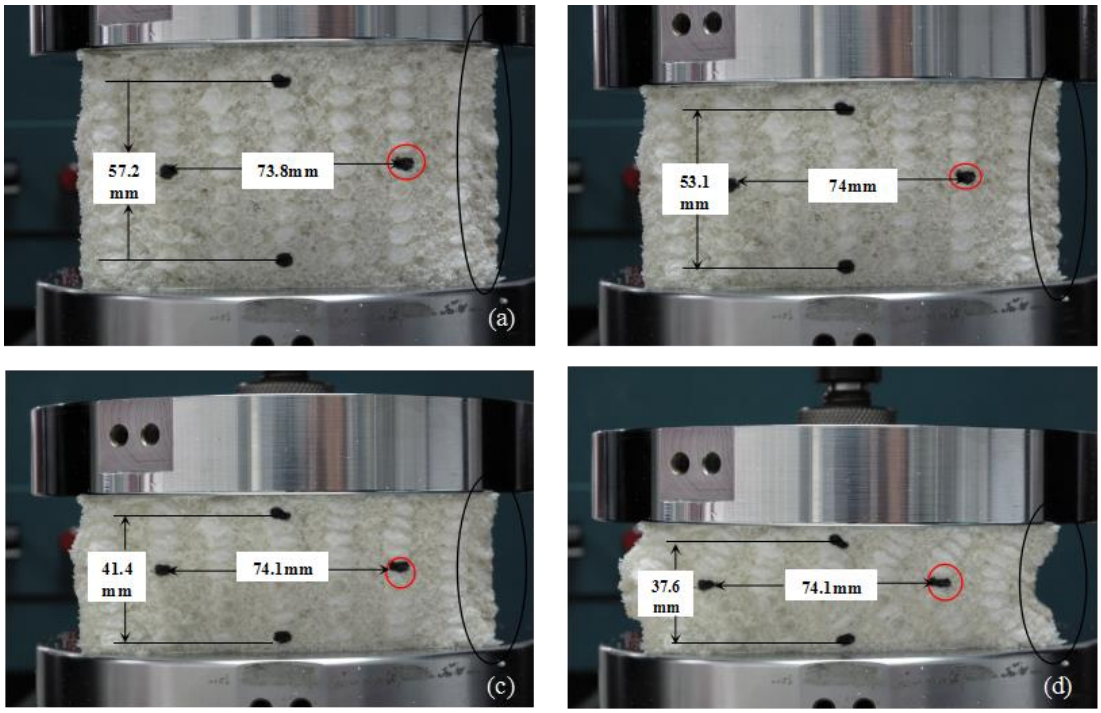

Figure 9 Lateral deformation of 6mm PPR non-auxetic composite under compression. Compression strain: (a) 0%; (b) 12.60%; (c) 42.39%; (d) 45.57%

Figure 10 shows the variation of the Poisson's ratio of auxetic composite 6mm NPR at different compression strains when subjected to repeated compression tests. It can be seen that the NPR values of the composite at all four compression strains decrease from the first compression cycle to the second one, but they tend to be stabilized after the second compression cycle. The result suggests that the retention of the auxetic effect of an auxetic composite is very important. The solution to increase the retention ability of the auxetic effect of a 3D textile composite might be to use foam with high elastic recovery ability to fabricate the matrix.

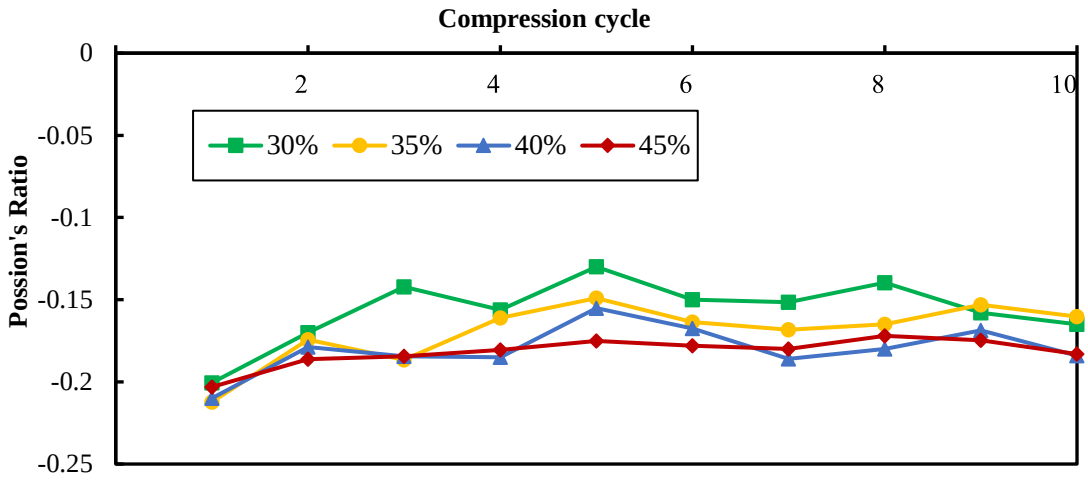

Figure 10 Variation of Poisson's ratio under repeated compression condition

3.2 Compression behavior

The compression stress-strain curves of the pure foam, auxetic composites and non-auxetic composites are shown in Figure 11. It can be seen that the compression curves of these three types of materials are very different. As shown in Figure 11, the pure PU foam, which is used as the matrix, has the lowest compression performance among the three types of materials. It has only a maximum value of $4.8x10^{-3}$MPa at the strain of 55%. Compared with composite materials, the pure PU foam behaves more flexible and has a larger deformation. However, the easy deformation of the PU foam under compression makes the auxetic composites easily shrunk in the lateral direction when compressed. As the arrangement of the warp yarns in the 3D auxetic textile structure allows the weft yarns to be easily bent in the x-z plane, the deformation of auxetic composites is much higher than that of non-auxetic composites under the same compression load, which indicates that the non-auxetic composites are much stiffer than the auxetic composites.

Compared to the compression behaviors of the non-auxetic and auxetic composites reported by Jiang and Hu et al. [24], the auxetic composites in this study have similar tendency, but the non-auxetic composites have different behaviors. The reason is that the materials used in two studies are different. Jiang used hollow ABS tubes as warp yarns which are more rigid and easier to be buckled under compression when they are arranged in a vertical line. However, in the current study, the braided yarns with lower bending modulus are used and their cross-sections are easy to be deformed under compression. Besides, the PU foam used in the previous study is much stiffer than the elastic compressible PU foam used in this study.

As shown in Figure 11, the compression stress-strain curves of auxetic composites can be generally divided into three stages according to the change of the slope of the curves. At the initial stage, a low slope is observed between the strain of 0% and 10% due to the compression of PU foam in gaps and outer layers and its ineffective constraint for the inner auxetic structure. When the composites are further compressed into the second stage ranging from 10% to 40%, the compression stress is very slowly increased and a quasi-plateau region is formed. The compression strain after 40% can be considered as the third stage. In this stage, the compression stress rapidly increases due to the compaction of the composite structure. Compared to the auxetic composites, the quasi-plateau region in the deformation of non-auxetic composites is not found. In this case, the deformation process could be divided into two stages. As shown in Figure 11, the first stage is a gradual increase of the compression stress from 0% to about 30% of compression strain, in which the change in the cross section of the warp

yarns from the circular form to the elliptic form could be visually observed. The second stage starts from about 30% of compression strain. In this stage, the compression stress rapidly increase and the warp yarns tend to get misaligned under compression. Although the test compression strain was set up to 55%, the compression tests were stopped before 55% as the compressive loads reached the capacity of the testing device. As arranged in a form of the vertical lines in the non-auxetic composite structures, the warp yarns play a critical role in bearing load during the compression process, which leads to a more rapid increase of the compression stress and a lower deformation of the non-auxetic composites. This arrangement also makes non-auxetic composite stiffer than the auxetic composite.

From Figure 11, it can be also found that the influence of warp yarn diameter on the compression behavior of composites is much less important than their arrangement in the textile structures. For the auxetic composites, as the warp yarns are not arranged in the form of vertical lines, the compression loads result in bending of the weft yarns in the initial stage and quasi-plateau stage. Therefore, the influence of warp yarn diameter is very low. However, the influence of the warp yarn diameter for the non-auxetic composites is more evident as the warp yarns withstand the compression load due to their arrangement in the form of the vertical lines. In this case, as the 6mm warp yarn is easier to get flattened than the 4mm warp yarn, the compression stress of the composite made of textile structure with 4mm warp yarn is higher than that of the composite made of textile structure with 6mm warp yarn within the same compression strain.

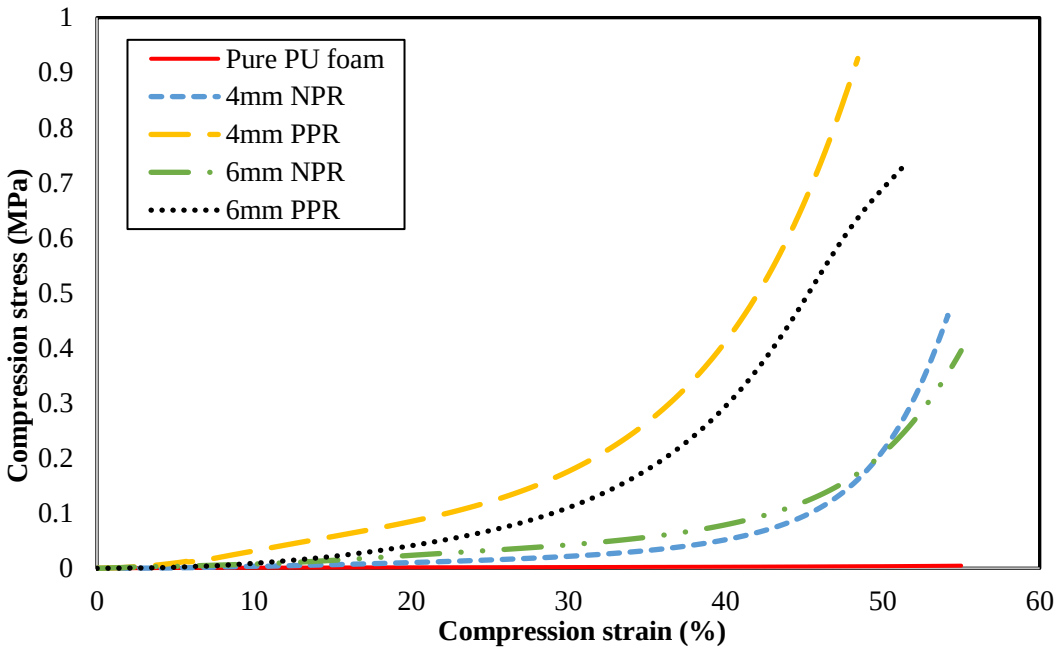

Figure 11 Compression stress-strain curves of pure PU foam, auxetic composites and non-auxetic composites

Figure 12 shows the compression stress-strain curves of the 4mm and 6mm auxetic composites under the repeated compression testing condition. It can be seen that the decline of compression stress of the composites after the first compression cycle is evident. After the first compression cycle, the compression behaviors of the composites tend to be stabilized. The similar behavior was observed for most of auxetic composites. The non-auxetic composites were not suitable for repeating compression test because the warp yarns would get misaligned when increasingly compressed. Actually, the retention of the compression behavior mainly depends on the elastic recovery of the PU foam. Therefore, to get a stable compression behavior of auxetic composite under repeating compression, PU foam with high elastic recovery is required.

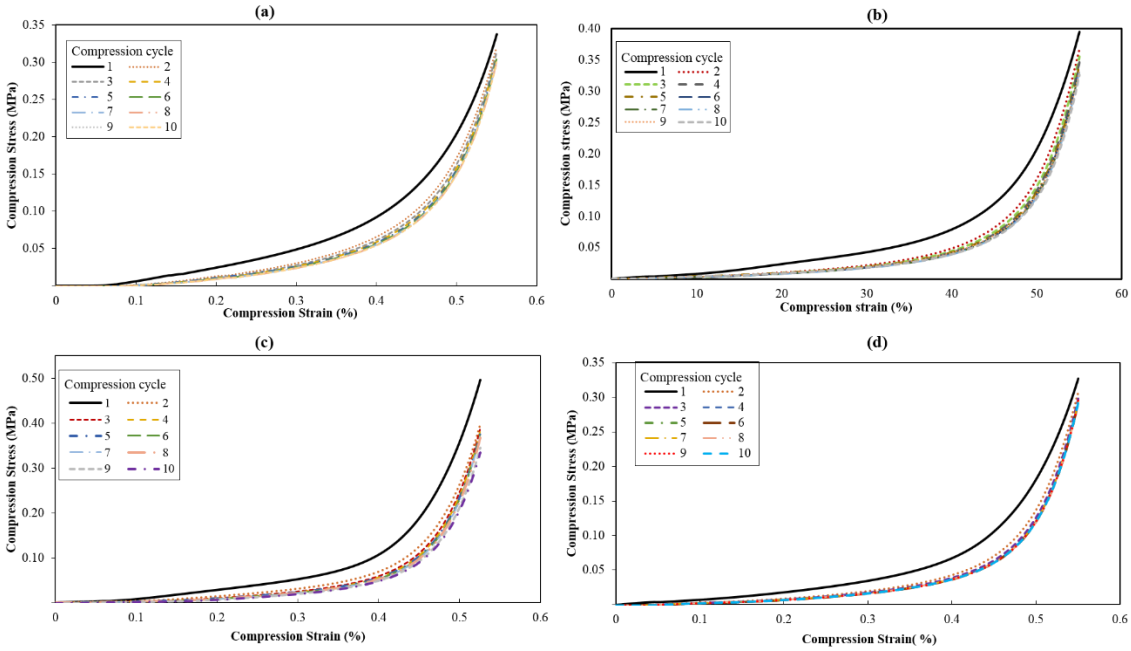

Figure 12 Compression stress-strain curves of auxetic composites under repeating compression condition (a) 6mm NPR sample 1; (b) 6mm NPR sample 2; (c) 4mm NPR sample 1; (d) 4mm NPR sample 2

4. Conclusion

A special type of auxetic composites were fabricated using 3D auxetic textile structure as reinforcement and PU foam as matrix via an injecting and foaming process. Their auxetic effect and compression behavior under compression were analyzed and compared with the pure PU foam and non-auxetic composites made with the same materials and structural parameters but with different warp yarn arrangement in textile structure. Based on the obtained results, one can draw the following conclusions:

1. It is possible to achieve NPR in a 3D textile structure if a suitable yarn arrangement is adopted. Auxetic composites can be easily produced using 3D auxetic textile structure as reinforcement and compressive foam as matrix.

2. The Poisson's ratios of the auxetic composite structures are not constant. They change with the compression strain and warp yarn diameter. The increase of the compression strain and warp yarn diameter can cause an increase of negative Poisson's ratio values. Pure PU foam, auxetic composites and non-auxetic composites all have zero Poisson's ratio in the initial stage of compression strain when compressed.
3. The auxetic composites and non-auxetic composites have different mechanical behaviors due to different arrangements of yarns in 3D textile structure. While the auxetic composite behaves more like a damping material with a lower range of compression stress, the non-auxetic composite behaves more like a stiffer material with a higher range of compression stress.
4. The deformation behavior and compression property of the auxetic composite tends to be stabilized after the first compression cycle under repeated compression testing condition.

Acknowledgement

The authors would like to thank the funding support from the Research Grants Council of Hong Kong Special Administrative Region Government in the form of a GRF project (No. 515812).

References

[1] Evans, K.E., Nkansah, M.A., Hutchinson, I.J., Rogers, S.C. (1991). Molecular network design. *Nature*, 353, 124.

[2] Lakes, R.S. (1987). Foam Structures with a Negative Poisson's Ratio. *Science*, 235, 1038-1040.

[3] Almgren, R.F. (1985). An isotropic three-dimensional structure with Poisson's ratio -1. *Journal of Elasticity*, 15, 427-430.

[4] Wojciechowski, K.W. (1987). Constant thermodynamic tension Monte Carlo studies of elastic properties of a two-dimensional system of hard cyclic hexamers. *Molecular Physics*, 61(5), 1247-1258.

[5] Alderson, K.L., Alderson, A., Smart, G., Simkins, V.R., & Davies, P.J. (2002). Auxetic polypropylene fibres: Part 1-manufacture and characterisation. *Plastics, Rubber and Composites*, 31, 344–349.

[6] Ravirala, N., Alderson, K.L., Davies, P.J., Simkins, V.R., & Alderson, A. (2006). Negative Poisson's ratio polyester fibers. *Textile Research Journal*, 76, 540-546.

[7] Simkins, V. R., Ravirala, N., Davies, P.J., Alderson, A., & Alderson, K.L. (2008). An experimental study of thermal post-production processing of auxetic polypropylene fibres. *physica status solidi (b)*, 245(3), 598-605

[8] Alderson, K., Alderson, A., Anand, S., Simkins, V., Nazare, S., & Ravirala, N. (2012). Auxetic warp knit textile structures. *physica status solidi (b)*, 249(7), 1322–1329.

[9] Ge, Z., & Hu, H. (2013). Innovative three-dimensional fabric structure with negative Poisson's ratio for composite reinforcement. *Textile Research Journal*, 83, 543–550.

[10] Ge, Z., Hu, H., & Liu, Y. (2013). A finite element analysis of a 3D auxetic textile

structure for composite reinforcement. *Smart Materials and Structures*, 22, 084005.

[11] Hu, H., Wang, Z., & Liu, S. (2011). Development of auxetic fabrics using flat knitting technology. *Textile Research Journal*, 81, 1493-1502.

[12] Wang, Z., & Hu, H. (2014). 3D auxetic warp- knitted spacer fabrics. *physica status solidi (b)*, 251(2), 281-288.

[13] Wang, Z., Hu, H., & Xiao, X. (2014). Deformation behaviors of 3D auxetic spacer fabrics. *Textile Research Journal*, 84, 17-28.

[14] Chan, N., & Evans, K.E. (1997). Fabrication methods for auxetic foams. *Journal of Materials Science*, 32, 5945-5953.

[15] Brandel, B., & Lakes, R.S. (2001). Negative Poisson's ratio polyethylene foams. *Journal of Materials Science*, 36(24), 5885-5893.

[16] Choi, J.B., & Lakes, R.S. (1992). Non-linear properties of polymer cellular materials with a negative Poisson's ratio. *Journal of Materials Science*, 27(17), 4678-4684.

[17] Lakes, R.S., & Elms, K. (1993). Indentability of conventional and negative Poisson's ratio foams. *Journal of Composite Materials*, 27(12), 1193-1202.

[18] Grima, J.N., Alderson, A., & Evans, K.E. (2005). An alternative explanation for the negative Poisson's ratios in auxetic foams. *Journal of the Physical Society of Japan*, 74(4), 1341-1342.

[19] Grima, J.N., Gatt, R., Ravirala, N., Alderson, A., & Evans, K.E. (2006). Negative Poisson's ratios in cellular foam materials. *Materials Science and Engineering*: A, 423(1), 214-218.

[20] Pozniak, A.A., Smardzewski, J., & Wojciechowski, K.W. (2013). Computer simulations of auxetic foams in two dimensions. *Smart Materials and Structures*, 22(8), 084009.

[21] Gatt, R., Attard, D., Farrugia, P.S., Azzopardi, K.M., Mizzi, L., Brincat, J.P., & Grima, J.N. (2013). A realistic generic model for anti-tetrachiral systems. *physica status solidi (b)*, 250(10), 2012-2019.

[22] Milton, G.W. (1992). Composite materials with Poisson's ratios close to -1. *Journal of the Mechanics and Physics of Solids*, 40(5), 1105-1137.

[23] Evans, K.E., Donoghue, J.P., & Alderson, K.L. (2004). The design, matching and manufacture of auxetic carbon fibre laminates. *Journal of Composite Materials*, 38, 95-106.

[24] Jiang, L., Gu, B., & Hu, H. (2016). Auxetic composite made with multilayer orthogonal structural reinforcement. *Composite Structures*, 135, 23-29

[25] Alderson, K.L., Simkins, V.R., Coenen, V.L., Davies, P.J., Alderson, A., & Evans, K.E. (2005). How to make auxetic fibre reinforced composites. *physica status solidi (b)*, 242(3), 509-518.

[26] Wojciechowski, K.W. (1989). Two-dimensional isotropic system with a negative Poisson ratio. *Physics Letters A*, 137(1), 60-64.

[27] Baughman, R.H., Shacklette, J.M., Zakhidov, A.A., & Stafström, S. (1998). Negative Poisson's ratios as a common feature of cubic metals. *Nature*, 392(6674), 362-365.

[28] Grima, J.N., et al. (2015). Tailoring Graphene to Achieve Negative Poisson's

Ratio Properties. *Advanced Materials*, 27(8), 1455-1459.

[29] Kimizuka, H., Kaburaki, H., & Kogure, Y. (2000). Mechanism for negative Poisson ratios over the α-β transition of cristobalite, SiO 2: a molecular-dynamics study. *Physical Review Letters*, 84(24). 5548.

[30] Tretiakov, K.V., & Wojciechowski, K.W. (2014). Partially auxetic behavior in fcc crystals of hard-core repulsive Yukawa particles. *physica status solidi (b)*, 251(2), 383-387.

[31] Strek, T., Maruszewski, B., Narojczyk, J.W., & Wojciechowski, K.W. (2008). Finite element analysis of auxetic plate deformation. *Journal of Non-Crystalline Solids*, 354(35), 4475-4480.

[32] Pozniak, A. A., Kaminski, H., Kedziora, P., Maruszewski, B., Strek, T., & Wojciechowski, K.W. (2010). Anomalous deformation of constrained auxetic square. *Rev. Adv. Mater. Sci*, 23, 169-174.

[33] Liu, Y., & Hu, H. (2010). A review on auxetic structures and polymeric materials. *Scientific Research and Essays*, (5), 1052-1063.

[34] Mir, M., Ali, M.N., Sami, J., & Ansari, U. (2014). Review of mechanics and applications of auxetic structures. *Advances in Materials Science and Engineering*, http://dx.doi.org/10.1155/2014/753496.

[35] Grima, J.N., Attard, D., Gatt, R., & Cassar, R.N. (2009). A Novel Process for the Manufacture of Auxetic Foams and for Their re-Conversion to Conventional Form. *Advanced Engineering Mater*ials, 11(7), 533-535.

[36] Evans, K.E., & Alderson, A. (2000). Auxetic materials: functional materials and

structures from lateral thinking!. *Advanced materials*, 12(9), 617-628.

[37] Milton, G.W. (1992). Composite materials with Poisson's ratios close to -1. *Journal of the Mechanics and Physics of Solids*, 40(5), 1105-1137.

[38] Herakovich, C.T. (1984). Composite laminates with negative through-the-thickness Poisson's ratios. *Journal of Composite Materials*, 18(5), 447-455.

[39] Peel, L.D. (2007). Exploration of high and negative Poisson's ratio elastomer-matrix laminates. *physica status solidi (b)*, 244(3), 988-1003.

[40] Chen, C.P., & Lakes, R.S. (1993). Viscoelastic behaviour of composite materials with conventional-or negative-Poisson's-ratio foam as one phase. *Journal of materials science*, 28(16), 4288-4298.

[41] Zhang, R., Yeh, H.L., & Yeh, H.Y. (1998). A preliminary study of negative Poisson's ratio of laminated fiber reinforced composites. *Journal of reinforced plastics and composites*, 17(18), 1651-1664.

[42] Hadi Harkati, E., Bezazi, A., Scarpa, F., Alderson, K., & Alderson, A. (2007). Modelling the influence of the orientation and fibre reinforcement on the Negative Poisson's ratio in composite laminates. *physica status solidi (b)*, 244(3), 883-892.

[43] Clarke, J.F., Duckett, R.A., Hine, P.J., Hucthinson, I.J., & Ward, I.M. (1994) Negative Poisson's ratios in angle-ply laminates: theory and experiment. *Composites* 1994; 25(9):863-8.

[44] Jayanty, S., Crowe, J., & Berhan, L. (2011). Auxetic fibre networks and their composites. *physica status solidi (b)*, 248(1), 73-81.

[45] Evans, K.E., Nkansah, M.A., & Hutchinson, I.J. (1992). Modelling negative Poisson ratio effects in network-embedded composites. *Acta metallurgica et materialia*, 40(9), 2463-2469.

[46] Miller, W., Hook, P.B., Smith, C.W., Wang, X., & Evans, K.E. (2009). The manufacture and characterisation of a novel, low modulus, negative Poisson's ratio composite. *Composites Science and Technology*, 69(5), 651-655.

[47] Ge, Z., Hu, H., & Liu, Y. (2015). Numerical analysis of deformation behavior of a 3D textile structure with negative Poisson's ratio under compression. *Textile Research Journal*, 2015, 85(5), 548-557

[48] Alderson, A., & Evans, K.E. (1997). Modelling concurrent deformation mechanisms in auxetic microporous polymers. *Journal of materials science*, 32(11), 2797-2809.

[49] Hu, H., & Zhang Z.K. (2015), A 3D auxetic fabric manufacturing device and method, Chinese invention patent, no. 20120192738.3, Beijing, State Intellectual Property Office of China.